Synthesis of Heat Exchanger Networks with Nonisothermal Phase Changes

M. M. Faruque Hasan, Gopalakrishnan Jayaraman, and I. A. Karimi
Dept. of Chemical & Biomolecular Engineering, National University of Singapore,
4 Engineering Drive 4, Singapore 117576

H. E. Alfadala
Dept. of Chemical Engineering, Qatar University, P.O. Box 2713, Doha, Qatar

DOI 10.1002/aic.12031
Published online September 29, 2009 in Wiley InterScience (www.interscience.wiley.com).

Most literature on the synthesis of heat exchanger networks via mathematical programming methods has dealt with phase changes by assuming nearly isothermal conditions. Many multicomponent phase changes of practical interest (e.g., those in sub-ambient processes) occur over ranges of temperatures and exhibit nonlinear temperature-enthalpy relations (T-H curve). In such cases, isothermal approximations may lead to inferior or unacceptable networks. In this article, we propose a mixed-integer nonlinear programming formulation and a solution algorithm to incorporate nonisothermal phase changes in heat exchanger network synthesis. We approximate the nonlinear T-H curves via empirical cubic correlations, and propose a procedure to ensure minimum temperature approach at all points in the exchangers. Our approach successfully solves two industry examples and shows promise for significant cost reductions when compared with existing processes. © 2009 American Institute of Chemical Engineers *AIChE J,* 56: 930–945, 2010

Keywords: process synthesis, heat integration, exchanger networks, phase change, mixed integer nonlinear programming (MINLP)

Introduction

Energy is a global concern. The industrial sector is the largest consumer of energy in the USA, which attributed nearly 32% of the total energy consumed in 2007.[1] As much as 40% of the total operational cost of a chemical plant is attributable to energy.[2] Limited crude oil reserves, high oil prices, tightening environmental regulations on CO_2 emissions, intense competition in an increasingly global market, etc. underline the importance of efficient use of energy. In fact, the cleanest energy is the one we never use. This is why energy integration has been a major concern in the chemical industry over the years.

Correspondence concerning this article should be addressed to I. A. Karimi at cheiak@nus.edu.sg.

Heat Exchanger (HE) Network Synthesis (HENS) is important for energy integration in chemical process plants. Given several hot and cold process streams and utilities with specified inlet and desired outlet temperatures, HENS involves the development of a network of HEs, heaters, and coolers with minimum annualized cost or another suitable objective. Since the first formulation by Masso and Rudd[3] in 1969, the HENS problem has been well studied. Gundersen and Naess,[4] Ježowski,[5,6] and Furman and Sahinidis[7] have given excellent reviews on HENS.

Figure 1 summarizes the past, present, and future of HENS literature. Past HENS work involved single-phase streams with linear temperature-enthalpy (*T-H*) relations. Furthermore, it mostly dealt with large temperature driving forces and ambient or above-ambient systems. In spite of the extensive literature on HENS, an optimization methodology for dealing with nonisothermal phase changes is missing.

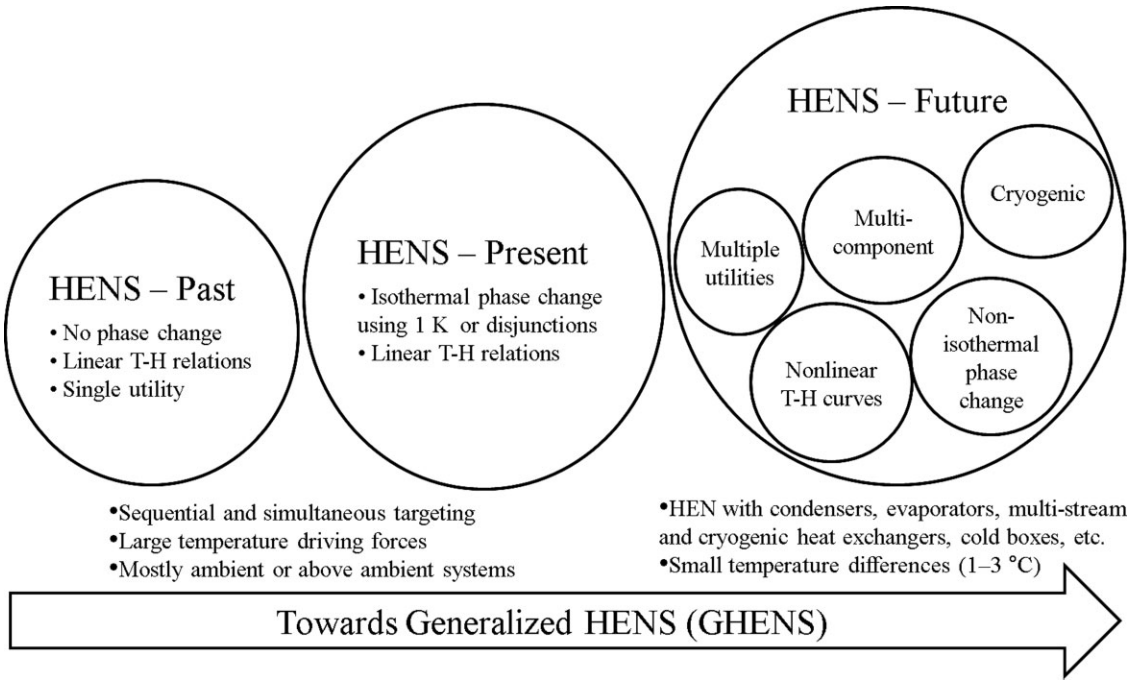

Figure 1. Past, present and future of HENS.

Although phase changes abound in industries such as petrochemicals, gas processing, cryogenic, and chemical, where operations such as distillation, stripping, refrigeration, etc. are common, the literature[8–10] on phase change in HENS is limited. A common approach[11] has been to assume the phase change to be isothermal and replace it by an "equivalent" sensible change with a fictitious heat capacity that gives the heat duty for the underlying phase change over 1 K. Clearly, such isothermal phase changes are possible for single-component streams and azeotrops only. The phase changes of most multicomponent mixtures span a range of temperatures and treating them as isothermal can be inaccurate. In subambient processes such as natural gas liquefaction and air enrichment, an accurate treatment of phase change is even more critical, because these processes operate with very small driving forces and even minute inaccuracies can have significant impact. Expensive utilities, liquefaction, evaporation, and energy-intensive refrigeration are common in such plants. However, the existing HENS literature does not accommodate units with nonisothermal phase changes, such as condensers, reboilers, evaporators, and multistream and multiphase cryogenic HEs for liquefaction and evaporation of mixtures.

Incorporating phase changes in GHENS (Generalized HENS or HENS-Future in Figure 1) poses several challenges. The first concerns the nonlinear and multizone *T-H* curves. A typical constant-pressure *T-H* curve for a subcritical multicomponent mixture has three distinct zones (gas, 2-phase, and liquid) partitioned by its bubble and dew point temperatures (BPT and DPT) as shown in Figure 2 for natural gas, which is a mixture of methane, ethane, propane, butane, and nitrogen. The shape and slope of the curve can vary markedly from one zone to another, and inflection points may be present. In contrast to $T \geq$ DPT and $T \leq$ BPT, where straight lines may be reasonable approximations, the curve is usually nonlinear for BPT $< T <$ DPT. In fact, the nonlinearity may occur even in 1-phase zones such as the near-critical region of a pure component or due to rapid changes in heat capacities as pointed out by Castier and Queiroz.[12] Certainly, a linear relation with a constant heat content rate, as in the traditional HENS, cannot describe even the individual zones of a *T-H* curve satisfactorily.

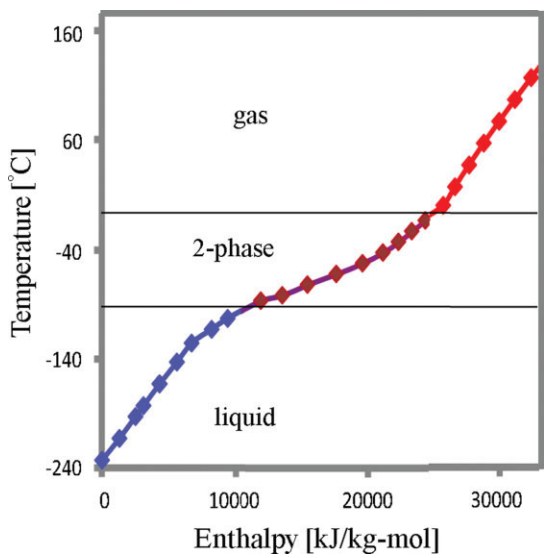

Figure 2. Temperature-enthalpy (*T-H*) curve for natural gas.

[Color figure can be viewed in the online issue, which is available at www.interscience.wiley.com.]

A nonlinear *T-H* curve poses an even more significant problem. The log mean temperature difference (LMTD) is no longer a valid driving force for computing the heat transfer area. In addition, we can no longer assume that the minimum temperature approach occurs only at one end of a HE, as it may occur anywhere internally. Ensuring that the minimum temperature approach condition holds at all points is challenging. These issues are even more critical for cryogenic processes, where the temperature driving forces are very small (1–3°C) and even a slight error can result in a large change in heat transfer area. For the case of a 1–2 condenser and cases where condensing curves have fronts or tails, the use of LMTD or FT $\times$ LMTD can result in prohibitively inaccurate HE areas,[13] or even an unacceptable HE.

The above challenges make HENS with nonisothermal phase changes a difficult problem. In this article, we present a MINLP model for GHENS or HENS with nonisothermal phase changes. Our model not only allows condensation and/or evaporation of mixtures, but also allows streams to transit through multiple states (gas, two-phase, and liquid) and incorporates multiple hot and cold utilities. We present a method for ensuring a minimum approach temperature (MAT) at all points in HEs and use average temperature driving forces to compute heat transfer areas for all streams including the phase-changing mixtures.

In what follows, we critically review the existing literature and state the GHENS problem. Next, we describe our modeling approach for nonlinear *T-H* relations and develop a MINLP formulation for GHENS. We then present an efficient iterative algorithm to solve large GHENS models, which commercial solvers fail to solve. Finally, we test our approach on several examples using real industrial case studies.

Previous Work

The existing work has used two approaches (sequential or simultaneous) for HENS. The former involves decomposing the problem into several subproblems with separate targets, while the latter addresses the full problem and all targets simultaneously. Three targets have been used in the literature.[14] These are minimum utility usage, fewest HE units, and minimum HE area or capital cost for the network. They are typically solved in the order stated. In this work, we will use a simultaneous approach based on mathematical programming.

The simultaneous approach formulates HENS as a single optimization problem that considers all targets simultaneously. Floudas and Ciric[15] proposed an MINLP formulation for the simultaneous targeting of fewest HE units and minimum exchanger areas based on a hyper-structure representation of the network. They combined the transshipment model[16] for fewest HEs with the network topology hyperstructure model[17] for the minimum area. Later, Ciric and Floudas[18] included the minimum utility cost target and formulated a single MINLP optimization problem to address all three targets simultaneously.

Yee and Grossmann[19] proposed another MINLP model (Synheat) for the simultaneous optimization of HENS. They assumed isothermal mixing. Although their objective function was nonlinear and nonconvex, they were able to obtain good solutions. Daichent and Grossmann[20] developed a preliminary screening procedure to reduce the superstructure by eliminating some suboptimal alternatives. Soršak and Kravanja[21] extended the superstructure to select HE types from several alternatives and used disjunctive programming. Most recently, Hasan et al.[22–24] applied a similar superstructure to model the operation of complex, proprietary, and multistream HEs.

The simultaneous approach for HENS results in an NP-hard problem[25] and nonconvexities often lead to local optima.[26] Several deterministic global optimization algorithms for the special/simplified versions of the model of Yee and Grossmann[19] are available in the literature. Zamora and Grossmann[27] developed thermodynamics-based convex underestimators and used them in their hybrid branch and bound/outer approximation algorithm to obtain global convergence under the simplifying assumptions of linear cost, arithmetic mean temperature differences, and no stream-splitting. Björk and Westerlund[28] presented a global optimization strategy by convexifying the signomial terms in the objective function. They also considered HENS with and without isothermal mixing. Recently, Bergamini et al.[29] developed piecewise underestimators for the nonconvex terms and applied an outer-approximation algorithm.

Nonisothermal phase changes

To the best of our knowledge, nonisothermal phase changes have attracted limited attention in the HENS literature. Recently, Ponce-Ortega et al.[9] extended the MINLP model of Yee and Grossmann[19] to address isothermal phase changes. They assumed constant sensible and latent heats for isothermal phase changes, and used disjunctions to model the entire *T-H* curve. Although this approach is reasonable for pure components and reduces complexity when dealing with mixtures, it may not be apposite for multicomponent mixtures with nondominating components and noncondensable gases. Castier and Queiroz[12] proposed a pinch-based methodology for the energy targeting problem in the presence of multicomponent phase changes. Liporace et al.[10] incorporated this methodology into the sequential HENS approach. However, none of these works considered the nonlinearity of the *T-H* curve within a given phase.

Hasan et al.[24] modeled multicomponent phase changes using a separate, nonlinear, empirical correlation for each zone (liquid, gas, 2-phase) of a *T-H* curve. However, they used binary variables to identify the prevailing stream states in their MINLP formulation. Because their goal was the operation of a multistream HE rather than the optimal design of a HEN, they did not address other challenges mentioned earlier for modeling phase changes in GHENS. In a follow-up work,[8] they showed that modeling phase-changes can reduce utility costs significantly in a network, but did not address issues related to minimum temperature driving force.

Problem Statement

A GHENS problem can be stated as follows. Given single/multiphase, single/multicomponent, hot/cold process streams and utilities, specified initial/final temperatures, compositions and flow rates, and cost data for exchangers (HEs,

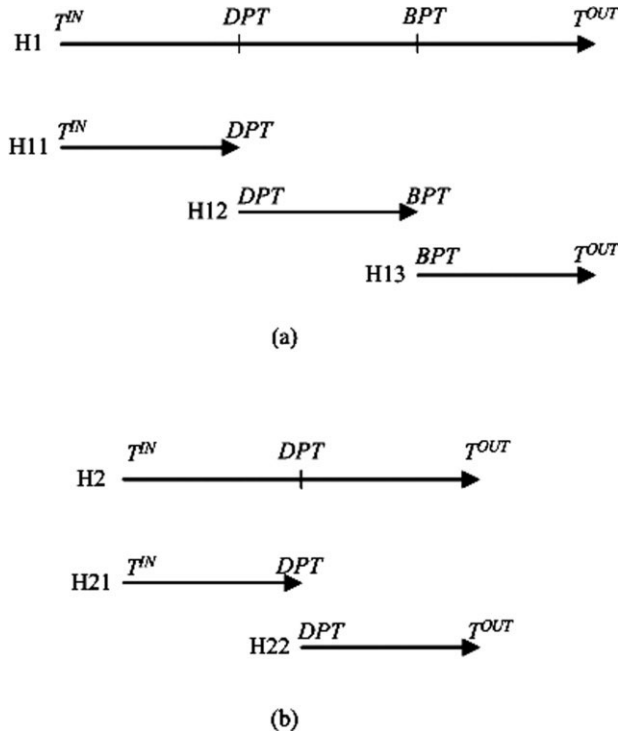

Figure 3. Decomposition of original multizone streams into single-zone sub-streams.

evaporators, condensers, heaters, and coolers) and utilities, develop a network of exchangers with minimum annualized cost or another suitable objective. Although it involves multizone (liquid, gas, 2-phase) streams, we convert it into and state it as the one involving single-zone streams only. In other words, we decompose each original (parent) multizone stream (both process and utility) into multiple single-zone streams. This is possible, since the BPT, DPT, and initial and final temperatures of each parent stream are known. For example, if a parent stream H1 (Figure 3a) transits through all three zones (gas, 2-phase, and liquid) while cooling down from an initial to a final temperature, then we replace H1 by three single-zone streams. One stream (H11) changes from the initial temperature to DPT, the second (H12) from DPT to BPT, and the third (H13) from BPT to the final temperature. Likewise, H2 (Figure 3b) transits through gas and 2-phase zones, so we replace it by H21 going from the initial temperature to DPT, and H22 from DPT to the final temperature. A single-zone parent stream remains as is. A similar approach for HENS was used by Liporace et al.,[10] but for sequential synthesis.

Although replacing each multizone stream by multiple single-zone streams enlarges the size of a GHENS problem, it enables us to assign a distinct single-zone *T-H* curve for each stream. This eliminates the need to use either binary variables[8,24] or disjunctions[9] to track applicable zones in a multizone stream. Because the heat transfer coefficients and *T-H* curve can vary drastically from zone to zone, modeling multizone streams is not easy and requires binary variables or disjunctions. Even from a practical perspective, single-zone streams may be desirable, as a separate exchanger of a different type may actually be used for each zone in reality. However, the resulting network with single-zone streams can be analyzed further to merge multiple HEs with the same pair of streams into one HE. A formulation with multizone exchangers is certainly possible. We intend to address it in near future.

GHENS involves two types of streams, process and utility. After replacing all multizone parent streams into single-zone streams, and using i for hot streams (process or utility), j for cold streams (process or utility), and s for any stream (hot or cold), we define the following sets.

$\mathbf{HP} = \{i \mid \text{Stream } i \text{ is a hot process stream}\}$
$\mathbf{HU} = \{i \mid \text{Stream } i \text{ is a hot utility stream}\}$
$\mathbf{CP} = \{j \mid \text{Stream } j \text{ is a cold process stream}\}$
$\mathbf{CU} = \{j \mid \text{Stream } j \text{ is a cold utility stream}\}$

Let $I = \text{Card}[\mathbf{HP}]$, $J = \text{Card}[\mathbf{CP}]$, $H = \text{Card}[\mathbf{HU}]$, $C = \text{Card}[\mathbf{CU}]$, and $K = \max[I, J]$, where Card[**X**] refers to the cardinality of set **X**. Let F_s be the mass flow rate of stream s. Note that the flows of all process streams are given, but those of utilities are unrestricted and unknown. Furthermore, the initial/final temperatures of all streams (process and utility) are known. With this, we revise our GHENS problem as follows.

Given the sets of hot/cold single-zone process streams with known flows; sets of hot/ cold single-zone utility streams with unknown and unrestricted flows and known costs; compositions, pressures, and initial/final temperatures of all streams; develop a HE network with minimum annualized cost or other suitable objective. We call this problem P and assume the following.

(1) The film heat transfer coefficient h_s for each stream s is a known constant. This will normally vary with flow rate, and this dependence needs to be addressed in the future.

(2) Heat transfer is countercurrent in each exchanger.

(3) Hot-to-hot and cold-to-cold matches are not allowed.

(4) Fouling and other thermal resistances are negligible and the overall heat transfer coefficient U_{ij} for a heat exchange between a hot stream i and cold stream j is $h_i h_j/(h_i + h_j)$.

(5) The operating cost of each utility varies linearly with the heat duty.

(6) Utilities are used only at extreme temperatures after exchanges with process streams are exhausted. However, our approach can accommodate utilities at each stage of our superstructure (described in the next section) by treating them as process streams with variable and unlimited flows.

We now present a MINLP formulation for P.

MINLP Formulation

We use a stage-wise superstructure based on that of Yee and Grossmann[19] to model all possible heat exchanges among hot and cold process streams. As shown in Figure 4 for a representative hot stream i and a cold stream j, our superstructure has $K + 2$ stages ($k = 0, 1,\ldots,K, K + 1$). Hot (cold) process streams enter stage $k = 1$ ($k = K$) and exit from stage $k = K + 1$ ($k = 0$). As in the existing HENS literature, the end stages ($k = 0$ and $k = K + 1$) are for exchange with utilities only, and intermediate stages ($k = 1$ through $k = K$) are for exchange between process streams only. In stage $k = 0$ ($k = K + 1$), hot (cold) utilities heat

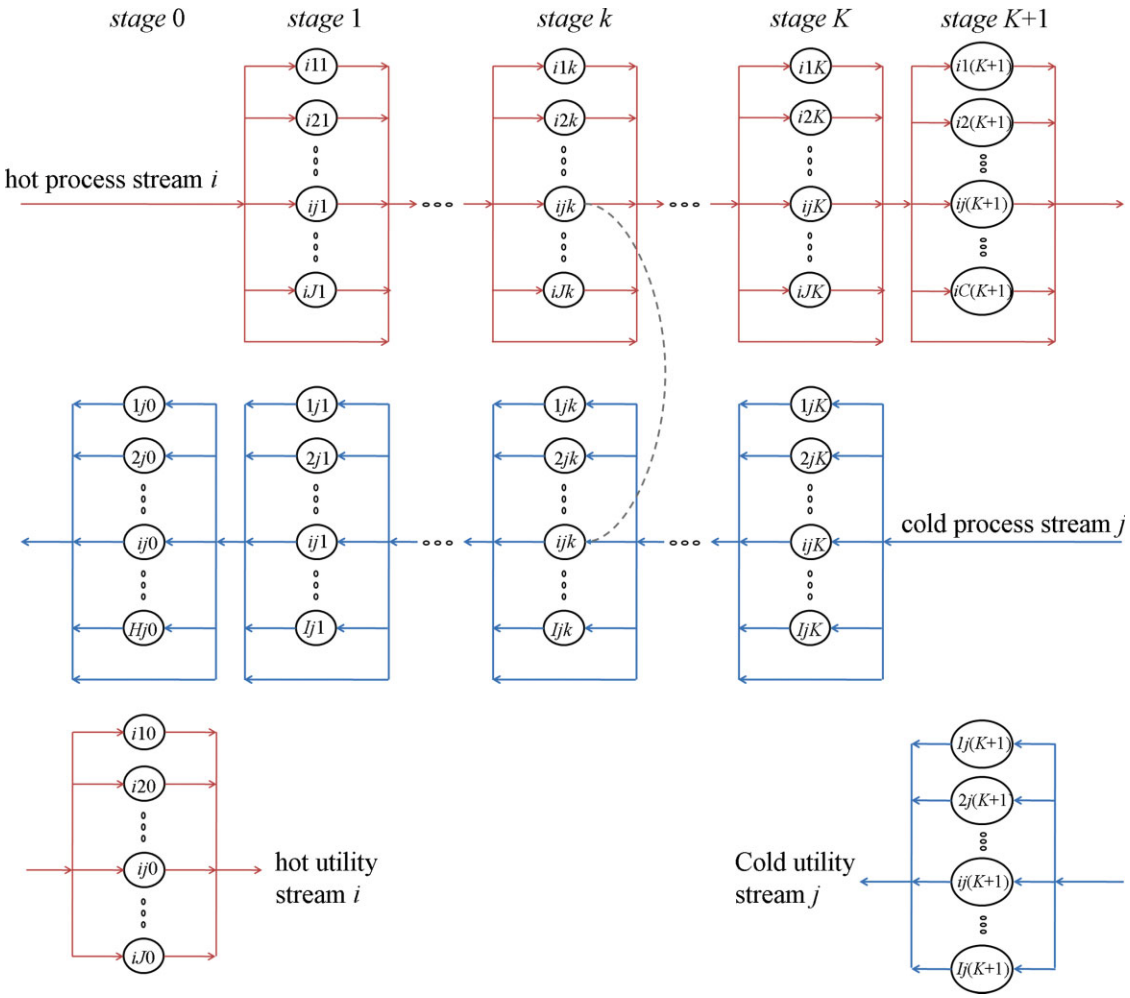

Figure 4. Stage-wise superstructure with representative process and utility streams.

[Color figure can be viewed in the online issue, which is available at www.interscience.wiley.com.]

(cool) the cold (hot) process streams. Each circle in the superstructure represents a possible exchanger. Each stage 1 through K has $I \times J$ possible exchangers, stage 0 has $J \times H$ heaters, and stage $(K + 1)$ has $I \times C$ coolers. On entering any stage, every process stream is split into multiple streams, one for each possible exchanger in that stage, and another for bypassing that stage fully. On leaving any stage, all splits of each stream combine to reform the original stream. The exchanger involving a split stream of hot stream i and that of a cold stream j in stage k is denoted as HE_{ijk}.

Our superstructure (Figure 4) is slightly more general than that of Yee and Grossmann.[19] First, it does not assume isothermal mixing. Second, it allows multiple utilities and nonlinear *T-H* relations for them. We believe this to be useful, as multiple utilities and multicomponent refrigerants are common in industries such as LNG plants, gas processing, air enrichment, etc. Third, it allows a stream to bypass any stage fully. Although we allow utilities at the extreme temperatures (stages 0 and $K + 1$) only in this work, our approach can accommodate them at every stage by simply treating them as process streams with variable unlimited flows. However, this increases model size, which discouraged us from doing it for our already difficult model. Note that the superstructure of Yee and Grossmann[19] misses some alternatives,[26] so ours does too.

GHENS involves three primary decisions: (1) existence of exchangers, (2) selection of stream splits, and (3) exchanger duties and areas. The existence of exchangers is addressed using the following binary variable (x_{ijk}, $k = 0, 1,\ldots,K, K + 1$).

$$x_{ijk} = \begin{cases} 1 & \text{if a split stream of hot stream } i \\ & \quad \text{contacts that of cold stream } j \text{ in stage } k \\ 0 & \text{otherwise} \end{cases}$$

Because stage 0 $(K + 1)$ does not involve any hot (cold) process stream, the valid ranges of i and j are: $i \in \mathbf{HU}$ for $k = 0$, $i \in \mathbf{HP}$ for $1 \le k \le K + 1$, $j \in \mathbf{CP}$ for $0 \le k \le K$, $j \in \mathbf{CU}$ for $k = K + 1$. Because k defines the domains of i and j unambiguously, we will no longer explicitly mention the domains of i and j. We will follow this practice consistently during the entire article.

To allow a stream s to bypass a stage k fully, we define the following 0–1 continuous variable.

$$y_{ik} = \begin{cases} 1 & \text{if stream } i \text{ bypasses stage } k \text{ fully} \\ 0 & \text{otherwise} \end{cases} \quad 1 \le k \le K+1$$

$$y_{jk} = \begin{cases} 1 & \text{if stream } j \text{ bypasses stage } k \text{ fully} \\ 0 & \text{otherwise} \end{cases} \quad 0 \le k \le K$$

Similarly, to detect the existence of a stage k, we define the following 0–1 continuous variable.

$$Y_k = \begin{cases} 1 & \text{if stage } k \text{ exists in the network} \\ 0 & \text{otherwise} \end{cases} \quad 1 \le k \le K$$

If a stream s bypasses a stage k, then no HE can exist for that stream in that stage, and vice versa. In other words,

$$y_{ik} + x_{ijk} \le 1 \quad 1 \le k \le K+1 \tag{1a}$$

$$y_{jk} + x_{ijk} \le 1 \quad 0 \le k \le K \tag{1b}$$

$$y_{ik} + \sum_{j=1}^{J} x_{ijk} \ge 1 \quad 1 \le k \le K+1 \tag{1c}$$

$$y_{jk} + \sum_{i=1}^{I} x_{ijk} \ge 1 \quad 0 \le k \le K \tag{1d}$$

The above equations ensure that y_{sk} will be binary automatically, and can be treated as 0–1 continuous variable.

If at least one stream passes through a stage, then the stage must exist. Moreover, if all streams bypass a stage, then the stage cannot exist. Therefore,

$$Y_k + y_{sk} \ge 1 \quad 1 \le k \le K \tag{2a}$$

$$Y_k + \sum_{s=1}^{S_k} y_{sk} \le S_k \quad 1 \le k \le K \tag{2b}$$

where, $S_k = H + J$ for $k = 0$, $S_k = I + J$ for $1 \le k \le K$, and $S_k = I + C$ for $k = K+1$. If a stage k exists, then all stages to its left must also exist.

$$Y_k \ge Y_{k+1} \quad 1 \le k \le K-1 \tag{3}$$

We have not seen Eqs. 1–3 or similar in previous HENS work. They eliminate redundant combinations in the superstructure and reduce computation time.

The second primary decision is to select stream splits. Let F_{ijk} and f_{ijk}, respectively, be the flow rates of the splits of streams i and j in HE_{ijk}. Therefore,

$$F_i y_{ik} + \sum_j F_{ijk} = F_i \quad 1 \le k \le K+1 \tag{4a}$$

$$F_j y_{jk} + \sum_i f_{ijk} = F_j \quad 0 \le k \le K \tag{4b}$$

The stream flow rates for a nonexistent exchanger must be zero. Furthermore, it may be advantageous to ensure minimum stream flows for existent exchangers. Thus,

$$F^{\text{L}}_{ijk} x_{ijk} \le F_{ijk} \le F_i x_{ijk} \quad 0 \le k \le K+1 \tag{5a}$$

$$f^{\text{L}}_{ijk} x_{ijk} \le f_{ijk} \le F_j x_{ijk} \quad 0 \le k \le K+1 \tag{5b}$$

where, F^{L}_{ijk} and f^{L}_{ijk} are the lower bounds.

The last primary decision involves exchanger duties. To compute the heat duty Q_{ijk} of HE_{ijk}, we must compute changes in the heat contents of streams. To this end, let T_{ik} (t_{jk}) be the temperature and H_{ik} (h_{jk}) be the enthalpy per unit mass of hot (cold) stream i (j) as it leaves (enters) stage k. At any point in the superstructure, only one stream type (process or utility) is present, except at points where process and utility streams leave/enter. To avoid the confusion between the temperatures of process vs. utility streams at the end stages, we rely on the domains of i and j defined unambiguously earlier to depend on k. However, to eliminate the confusion fully, let TIN_s (TOUT_s) be the in (out) temperature of stream s with enthalpy HIN_s (HOUT_s). In other words, $T_{i0} = \text{TOUT}_i$ ($i \in \mathbf{HU}$, since $k = 0$), and t_{jK} is the temperature of cold process stream j as it enters stage K, since $j \in \mathbf{CP}$ for $0 \le k \le K$. Then, we define the lowest temperature of each stream as the reference temperature for computing enthalpy. Thus, the reference temperatures are $T_{i(K+1)}$ for $i \in \mathbf{HP}$, T_{i0} for $i \in \mathbf{HU}$, t_{jK} for $j \in \mathbf{CP}$, and $t_{j(K+1)}$ for $j \in \mathbf{CU}$. Consequently, $H_{i(K+1)} = H_{i0} = h_{jK} = h_{j(K+1)} = 0$. With that, an energy balance across each stage gives,

$$\text{HIN}_i \sum_j F_{ij0} = \sum_j Q_{ij0} \tag{6a}$$

$$F_i(\text{HIN}_i - H_{i1}) = \sum_j Q_{ij1} \tag{6b}$$

$$F_i\left(H_{i(k-1)} - H_{ik}\right) = \sum_j Q_{ijk} \quad 2 \le k \le K+1 \tag{6c}$$

$$F_j\left(\text{HOUT}_j - h_{j0}\right) = \sum_i Q_{ij0} \tag{6d}$$

$$F_j\left(h_{j(k-1)} - h_{jk}\right) = \sum_i Q_{ijk} \quad 1 \le k \le K \tag{6e}$$

$$\text{HOUT}_j \sum_i f_{ij(K+1)} = \sum_{\text{i}} Q_{ij(K+1)} \tag{6f}$$

Let ΔH_{ijk} and Δh_{ijk} be the changes in enthalpies per unit mass for hot stream i and cold stream j in HE_{ijk}. Clearly,

$$Q_{ijk} = F_{ijk}\Delta H_{ijk} = f_{ijk}\Delta h_{ijk} \tag{7a, b}$$

The bounds for Q_{ijk}, H_{ik}, h_{jk}, ΔH_{ijk}, and Δh_{ijk} are $0 \le Q_{ijk} \le \min[F_i\text{HIN}_i, F_j\text{HOUT}_j]$, $0 \le (H_{ik}, \Delta H_{ijk}) \le \text{HIN}_i$, and $0 \le (h_{jk}, \Delta h_{ijk}) \le \text{HOUT}_j$. To ensure that the changes in the unit enthalpies of streams are zero for a nonexistent HE, we use,

$$\Delta H_{ijk} \le \text{HIN}_i x_{ijk} \tag{8a}$$

$$\Delta h_{ijk} \le \text{HOUT}_j x_{ijk} \tag{8b}$$

To ensure that the changes in unit enthalpies do not cross HIN_i (HOUT_j) for hot (cold) stream i (j) at any stage, we apply,

$$\Delta H_{ijk} \le H_{i(k-1)} \tag{9a}$$

$$h_{jk} + \Delta h_{ijk} \le \mathrm{HOUT}_j \tag{9b}$$

As discussed earlier, ensuring a minimum temperature difference at all points in each exchanger is a significant challenge, when the *T-H* profiles are nonlinear. We now address this critical issue.

Minimum approach temperatures

To ensure a MAT, we must compute temperature approach at all points in an exchanger. This is why we express temperature (T) as a function of enthalpy (H) instead of using the conventional approach of expressing H as a function of T. This approach has an advantage, as we do not use temperature at all in our formulation. Although it may be possible to derive highly nonlinear and complex analytical expressions for H vs. T using thermodynamic property packages or correlations, it is not possible to do so for T vs. H. In other words, we must use an empirical correlation or piecewise linear approximation for T vs. H. Although the latter is simple to develop, solving a GHENS model using that approach needs further work, which is beyond the scope of this article. Therefore, we preferred the former approach in this work. To avoid highly nonlinear and complex expressions and still allow inflection points, cubic correlations seemed the simplest possible option. Therefore, with no loss of generality, we assume the following empirical cubic correlation for each zone in the *T-H* curve for each stream.

$$T_i = T_{i(K+1)} + A_i[H_i] + B_i[H_i]^2 + C_i[H_i]^3 \quad i \in \mathbf{HP} \tag{10a}$$

$$T_i = T_{i0} + A_i[H_i] + B_i[H_i]^2 + C_i[H_i]^3 \quad i \in \mathbf{HU} \tag{10b}$$

$$t_j = t_{jK} + A_j[h_j] + B_j[h_j]^2 + C_j[h_j]^3 \quad j \in \mathbf{CP} \tag{10c}$$

$$t_j = t_{j(K+1)} + A_j[h_j] + B_j[h_j]^2 + C_j[h_j]^3 \quad j \in \mathbf{CU} \tag{10d}$$

where, A_s, B_s, and C_s are parameters fitted for stream s using suitable constant-pressure *T-H* data.

When *T-H* profiles are linear, as assumed by the existing HENS work, MAT occurs at one end of an exchanger. However, when they are nonlinear, we must identify the point along the exchanger, where MAT occurs and then demand MAT $\ge \theta$, where θ is the specified MAT. Let z_{ijk} ($0 \le z_{ijk} \le 1$) denote an internal point in HE_{ijk} such that $z_{ijk}\Delta H_{ijk}$ is the amount of heat exchanged from the entry ($z_{ijk} = 0$) of the hot stream to z_{ijk}. Let $\psi(z_{ijk}) = T(z_{ijk}) - t(z_{ijk})$ denote the temperature approach at z_{ijk}, where $T(z_{ijk})$ is the hot stream and $t(z_{ijk})$ is the cold stream temperature at z_{ijk}. From Eq. 10a–d, we obtain $\psi(z_{ijk})$ as:

$$\begin{aligned}\psi(z_{ijk}) = {} & \mathrm{TR}_i + A_i\left(H_{i(k-1)} - z_{ijk}\Delta H_{ijk}\right) \\ & + B_i\left(H_{i(k-1)} - z_{ijk}\Delta H_{ijk}\right)^2 + C_i\left(H_{i(k-1)} - z_{ijk}\Delta H_{ijk}\right)^3 \\ & - \mathrm{TR}_j - A_j\left[h_{jk} + \left(1 - z_{ijk}\right)\Delta h_{ijk}\right] \\ & - B_j\left[h_{jk} + \left(1 - z_{ijk}\right)\Delta h_{ijk}\right]^2 - C_j\left[h_{jk} + \left(1 - z_{ijk}\right)\Delta h_{ijk}\right]^3\end{aligned} \tag{11}$$

where, $TR_i = T_{i0}$ and $H_{i(k-1)} = \mathrm{HIN}_i$ for $i \in \mathbf{HU}$, $TR_i = T_{i(K+1)}$ for $i \in \mathbf{HP}$, $TR_j = t_{jK}$ for $j \in \mathbf{CP}$ and $TR_j = t_{j(K+1)}$ and $h_{jk} = \mathrm{HIN}_j$ for $j \in \mathbf{CU}$. We express $\psi(z_{ijk})$ as the following cubic polynomial in z_{ijk}.

$$\psi(z_{ijk}) = a_{ijk} + b_{ijk}z_{ijk} + c_{ijk}z_{ijk}^2 + d_{ijk}z_{ijk}^3 \tag{12}$$

where, a_{ijk}, b_{ijk}, c_{ijk}, and d_{ijk} are given by,

$$\begin{aligned}a_{ijk} = {} & \mathrm{TR}_i + A_iH_{i(k-1)} + B_iH_{i(k-1)}^2 + C_iH_{i(k-1)}^3 \\ & - \left[\mathrm{TR}_j + A_j\left(h_{jk} + \Delta h_{ijk}\right) + B_j\left(h_{jk} + \Delta h_{ijk}\right)^2 + C_j\left(h_{jk} + \Delta h_{ijk}\right)^3\right]\end{aligned} \tag{13a}$$

$$\begin{aligned}b_{ijk} = {} & \left[A_j + 2B_j\left(h_{jk} + \Delta h_{ijk}\right) + 3C_j\left(h_{jk} + \Delta h_{ijk}\right)^2\right]\Delta h_{ijk} \\ & - \left[A_i + 2B_iH_{i(k-1)} + 3C_iH_{i(k-1)}^2\right]\Delta H_{ijk}\end{aligned} \tag{13b}$$

$$\begin{aligned}c_{ijk} = {} & \left[B_i + 3C_iH_{i(k-1)}\right]\Delta H_{ijk}^2 \\ & - \left[B_j + 3C_j\left(h_{jk} + \Delta h_{ijk}\right)\right]\Delta h_{ijk}^2\end{aligned} \tag{13c}$$

$$d_{ijk} = C_j\Delta h_{ijk}^3 - C_i\Delta H_{ijk}^3 \tag{13d}$$

Appendix derives the analytical constraints that identify the point of MAT in HE_{ijk}. These MAT constraints, which must hold when HE_{ijk} exists, are as follows.

$$a_{ijk} \ge \theta_{ijk}x_{ijk} - M_{ijk}\left(1 - x_{ijk}\right) \tag{14a}$$

$$a_{ijk} + b_{ijk} + c_{ijk} + d_{ijk} \ge \theta_{ijk}x_{ijk} - M_{ijk}\left(1 - x_{ijk}\right) \tag{14b}$$

$$c_{ijk}^2 - 3b_{ijk}d_{ijk} \le M_{ijk1}\alpha_{ijk1} \tag{14c}$$

$$-b_{ijk} \le M_{ijk2}\alpha_{ijk2} \tag{14d}$$

$$b_{ijk} + 2c_{ijk} + 3d_{ijk} \le M_{ijk3}\alpha_{ijk3} \tag{14e}$$

$$\begin{aligned}& 9d_{ijk}\left(3a_{ijk}d_{ijk} - b_{ijk}c_{ijk}\right) + 2c_{ijk}^3 - 2\left(c_{ijk}^2 - 3b_{ijk}d_{ijk}\right)^{3/2} \\ & - 27\theta_{ijk}d_{ijk}^2 \le M_{ijk}\left(\alpha_{ijk1} + \alpha_{ijk2} + \alpha_{ijk3} - 2x_{ijk}\right)\end{aligned} \tag{14f}$$

where, θ_{ijk} is the specified MAT for HE_{ijk}; M_{ijk}, M_{ijk1}, M_{ijk2}, and M_{ijk3} are sufficiently large numbers; and α_{ijk1}, α_{ijk2}, and α_{ijk3} are the binary variables defined below.

$$\alpha_{ijk1} = \begin{cases} 1 & \text{if } c_{ijk}^2 \ge 3b_{ijk}d_{ijk} \\ 0 & \text{otherwise} \end{cases}$$

$$\alpha_{ijk2} = \begin{cases} 1 & \text{if } b_{ijk} \le 0 \\ 0 & \text{otherwise} \end{cases}$$

$$\alpha_{ijk3} = \begin{cases} 1 & \text{if } b_{ijk} + 2c_{ijk} + 3d_{ijk} \ge 0 \\ 0 & \text{otherwise} \end{cases}$$

Appendix also gives a possible set of values for M_{ijk}, M_{ijk1}, M_{ijk2}, and M_{ijk3}.

Heat exchanger areas

Since $\psi(z_{ijk})$ is nonlinear, we cannot use LMTD (Log Mean Temperature Difference) to compute the exchanger areas. Lee et al.[30] divided the entire *T-H* curve into several segments, assumed a linear approximation for each segment, and used LMTD to compute a separate heat transfer area for each segment. Computing area by integrating the fundamental heat transfer equation is nearly impossible, so we use an average temperature difference (ATD_{ijk}) instead of LMTD for HE_{ijk}. In other words,

$$\mathrm{ATD}_{ijk} = \int_0^1 \psi\left(z_{ijk}\right) dz_{ijk} \tag{15}$$

For our proposed cubic *T-H* correlation, ATD_{ijk} is given by,

$$\mathrm{ATD}_{ijk} \le a_{ijk} + \frac{b_{ijk}}{2} + \frac{c_{ijk}}{3} + \frac{d_{ijk}}{4} + M_{ijk}\left(1 - x_{ijk}\right) \tag{16}$$

Note that Eq. 16 can be an inequality, since the objective is to minimize the cost, which decreases with ATD. Since ATD_{ijk} is an average, we can safely use $\theta_{ijk} \le \mathrm{ATD}_{ijk} \le \max[\theta_{ijk}, \mathrm{TIN}_i - \mathrm{TIN}_j]$. Note that Eq. 14a-f force x_{ijk} to be zero, when the MAT conditions cannot be met.

Network synthesis objective

Our objective is to minimize the annualized cost of the network, which is the sum of the fixed costs of the HEs, the cost of utilities, and the cost of exchanger areas. This is given by,

$$\text{Minimize } \sum_i \sum_j \sum_k \mathrm{FC}_{ij} x_{ijk} + \sum_i \sum_j \mathrm{UC}_i Q_{ij0} + \sum_i \sum_j \mathrm{UC}_j Q_{ij(K+1)} + \sum_i \sum_j \sum_k \mathrm{CA}_{ij} \left[\frac{Q_{ijk}}{U_{ij}\mathrm{ATD}_{ijk}}\right]^{\eta_{ij}} \tag{17}$$

where, FC_{ij} and CA_{ij} are the fixed costs of installation and cost of unit area of the exchanger between stream i and j, UC_s is the unit cost of utility s, and η is the exponent of area cost relation and usually positive.

This completes our MINLP formulation (F0) that involves Eqs. 1–9, 13 and 14, and 16 and 17. After solving the model, we obtain the temperatures of all streams from their heat contents.

Solution Strategy

F0 is a nonconvex MINLP. It is significantly larger and more complex than the existing HENS formulations due to the highly nonlinear and nonconvex energy balances and MAT constraints. Thus, solving F0 even for a few streams is difficult. Commercial solvers such as GAMS/DICOPT[31] and GAMS/BARON[32] fail to make progress or end with infeasibility. Thus, we need a special strategy to get a good solution to this difficult problem.

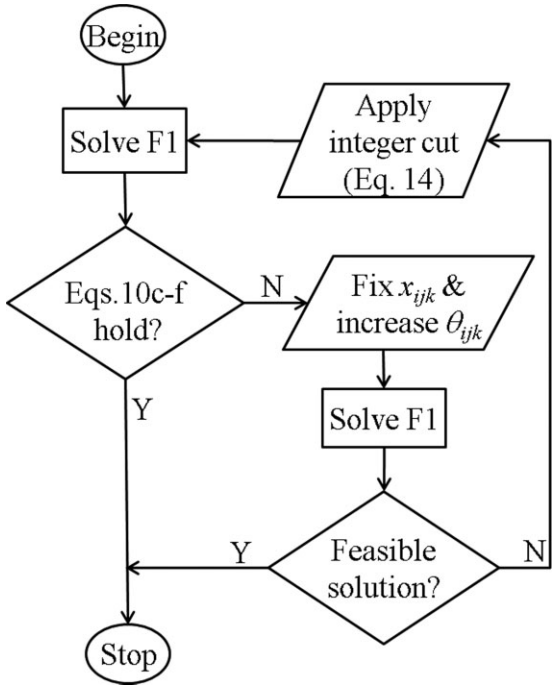

Figure 5. Algorithm for solving large problems.

Our first simplification arises from the fact that Eq. 14c–f must hold, only when $x_{ijk} = 1$. In other words, for the sake of simplifying the problem, and getting a solution, one could eliminate Eq. 14c–f. To this end, we define F1 as F0 without Eq. 14c–f. An arbitrary feasible solution to F1 is also feasible for F0, if Eq. 14c–f hold for every exchanger in that solution. Therefore, we solve F1 instead of F0 in our algorithm (Figure 5). Once we get a solution (say *S*) from F1, we check if Eq. 14c–f hold. If they do, then we have a solution to F0. If they do not, then *S* is infeasible for F0, and must be repaired. However, the infeasibility of *S* does not mean that the network configuration given by *S* is also infeasible. We can adjust the stream temperatures and exchanger duties in *S* to ensure MAT. Therefore, we fix the network configuration, and solve F1 again, but with some higher values of θ_{ijk}. The basic idea is to increase the temperature driving forces sufficiently at both ends so that MAT $\ge \theta_{ijk}$ at all points in HE_{ijk}. A solution obtained in this manner would satisfy Eq. 14c–f and would be a feasible solution to F0. If no such feasible solution can be obtained, then we can eliminate this configuration from subsequent consideration by adding the following well-known integer cut.

$$\sum_{(i,j,k)\ni[x_{ijk}]=1} x_{ijk} \le \left(\sum_i \sum_j \sum_k [x_{ijk}]\right) - 1 \tag{18}$$

where, $[x_{ijk}]$ is the value of x_{ijk} in the infeasible *S*. We continue the above procedure, until we have a feasible network for F0. This completes our algorithm.

F1 should be easier to solve than F0, as it does not have α_{ijk1}, α_{ijk2}, α_{ijk3}, and Eq. 14c–f. However, good starting points seem crucial. GAMS[33] provides an option to generate and try several random initial points. For small problems

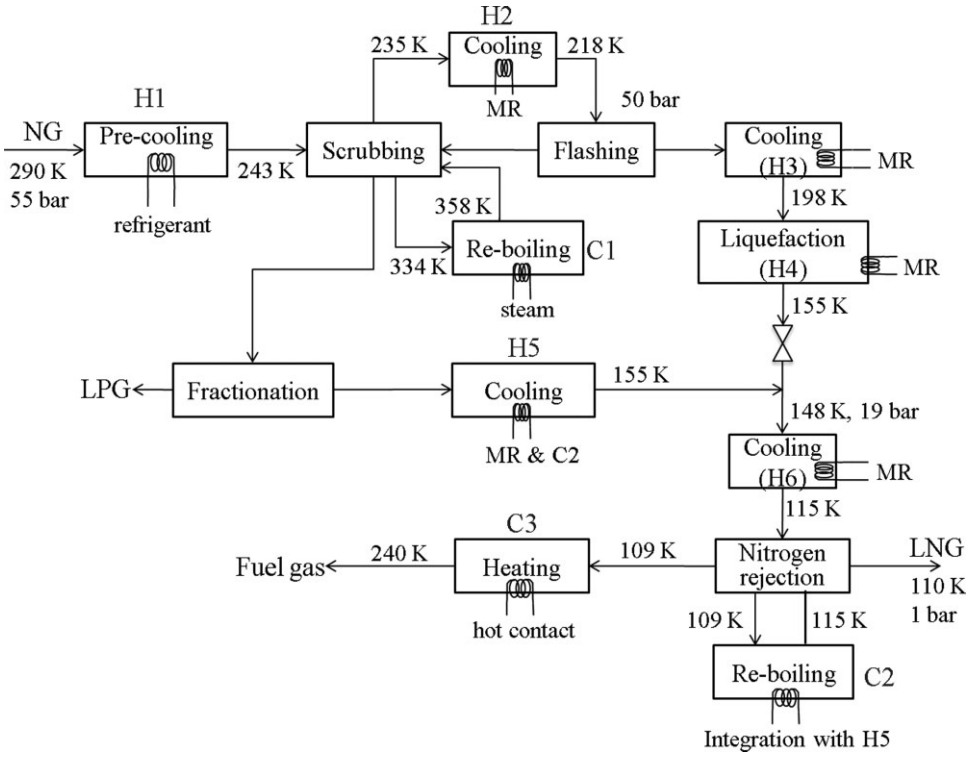

Figure 6. Flow diagram of LNG plant.

with a few streams, it may be possible to devise a feasible network for the starting point. For large problems, one may use a network with heaters and coolers only (without any heat integration) as the starting point. Such a network can be derived without optimization by simply assigning appropriate utilities to each process stream to achieve the desired temperature change. However, BARON and DICOPT fail to improve such a network. Therefore, to obtain a starting network for the algorithm, we replace Eq. 7a,b by the following convex and concave relaxations and solve F0.

$$Q_{ijk} \geq F_{ijk}\mathrm{HIN}_i + F_i\Delta H_{ijk} - F_i\mathrm{HIN}_i \tag{19a}$$

$$Q_{ijk} \leq F_{ijk}\mathrm{HIN}_i \tag{19b}$$

$$Q_{ijk} \leq F_i\Delta H_{ijk} \tag{19c}$$

$$Q_{ijk} \geq f_{ijk}\mathrm{HOUT}_j + F_j\Delta h_{ijk} - F_j\mathrm{HOUT}_j \tag{19d}$$

$$Q_{ijk} \leq f_{ijk}\mathrm{HOUT}_j \tag{19e}$$

$$Q_{ijk} \leq F_j\Delta h_{ijk} \tag{19f}$$

Since Eq. 19a–f reduce the possibility of an infeasible network, we add these constraints to F0 at all subsequent steps along with Eq. 7a,b.

Examples

We use two real-life case studies to illustrate the application of our model and solution approach. The first study involves a cryogenic process to produce LNG, and the second a petrochemical process to purify phenol. The computing platform is a Dell Precision AW-T7400 with Quad-Core Intel® Xeon® X5492 (3.4 GHz) Processor, 64 GB of RAM using CPLEX v.11 (LP solver), CONOPT v.3 (NLP solver), BARON (MINLP solver), and DICOPT (MINLP solver) in GAMS 22.8. We used *T-H* data from Aspen HYSYS 2004.2 to compute the parameters for the cubic correlations. We used Eq. A7 to compute the big-*M* values for these two examples.

LNG plant

LNG is the cleanest fossil fuel and the most economic means of transporting natural gas (NG) over long distances. However, NG liquefaction is an energy-intensive process. That is why LNG industry[23–24,,30,34–38] is practicing optimization increasingly. It is also an ideal case for GHENS. The LNG process is cryogenic, and involves multicomponent phase changes, multiple utilities, and multistream HEs[24] with small temperature driving forces.[30] Figure 6 shows the flow diagram for a base-load LNG plant. It involves five hot and three cold parent streams. One hot stream passes through two states, namely gas and two-phase. We decompose it into two sub-streams using its dew point. This gives us six hot (H1-6) and three cold (C1-C3) process streams. Two hot (H7-8) and two cold utilities (C4-5) are also available. C5 is a mixture and is called mixed-refrigerant (MR). Table 1 gives the flows, temperatures, enthalpies, film heat transfer coefficients, and stream property data. H1 and H2 are NG streams that require pre-cooling. H3 and H4 are pre-cooled NG streams that are to be liquefied completely. These are the two sub-streams created from one parent hot stream. All

Table 1. Stream Data for the LNG Plant

Stream	Flow Rate (Mmol/h)	Initial Temperature (K)	Final Temperature (K)	Total Enthalpy Change (100 MJ/Mmol)	h (KJ/sm^2 K)	Fitted Parameters		
						A	B	C
HI	25.900	290	243	24.00	1.2	2.04209578	0.02863706	−0.00133863
H2	24.700	235	218	10.70	2	1.75758677	−0.00678138	−0.00084061
H3	23.300	218	198	34.30	2	1.27488386	−0.0340836	0.00040568
H4	23.300	198	155	39.20	2	0.45958176	0.02070552	−0.00011343
H5	0.5250	269	155	105.0	2	0.74430996	0.00866792	−0.00005159
H6	23.825	148	115	19.50	2	1.57087207	0.00916536	−0.00015066
H7	–	450	440	6.400	0.2222	2.0705201	−0.03414313	−0.00706797
H8	–	370	365	4.400	0.2162	1.37717748	−0.05418563	−0.00012381
CI	0.6350	334	358	10.10	1	2.95083385	−0.0815781	0.0024443
C2	25.000	109	115	11.85	0.8283	0.54713808	−0.00026286	−0.00026843
C3	25.680	109	240	40.50	1.1441	3.18310153	0.00353632	−0.00005594
C4	–	140	160	25.00	0.2	0.85941461	−0.00947259	0.00028384
C5	–	105	110	2.800	0.1225	1.63395675	0.16259944	−0.0387144

hot and cold process and utility streams are multicomponent mixtures that may undergo nonisothermal phase changes. H4, H5, C1, and C2 undergo complete phase change. In practice, all hot streams use costly refrigeration (e.g., MR), and all cold streams except C2 use steam to attain their final temperatures. A portion of H5 is used to reboil C2.

The maximum *T-H* prediction error (Figure 7) using cubic correlations for all streams and utilities is ±1.2%. As shown

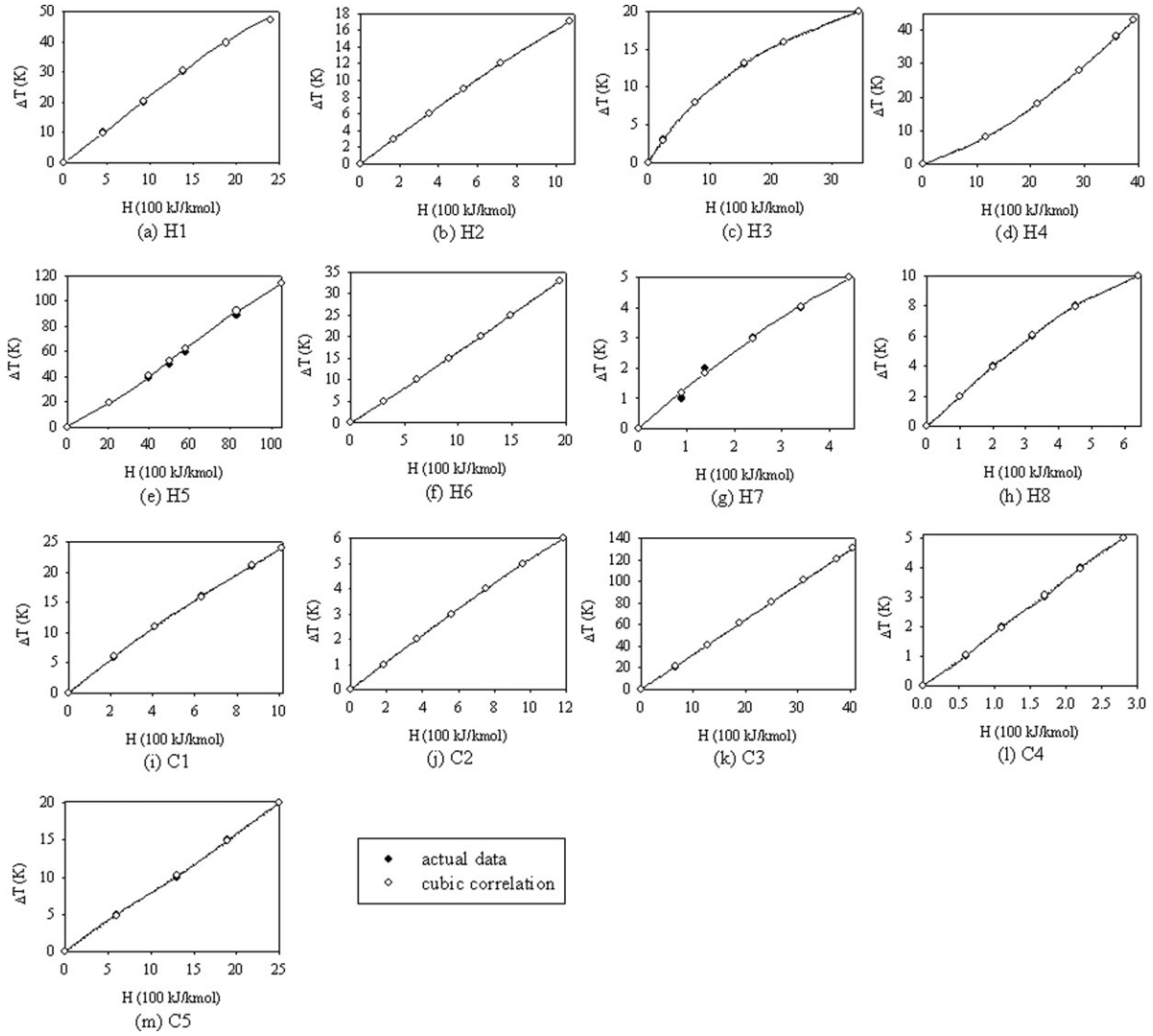

Figure 7. Actual *T-H* curves vs. cubic approximations for streams in the LNG plant.

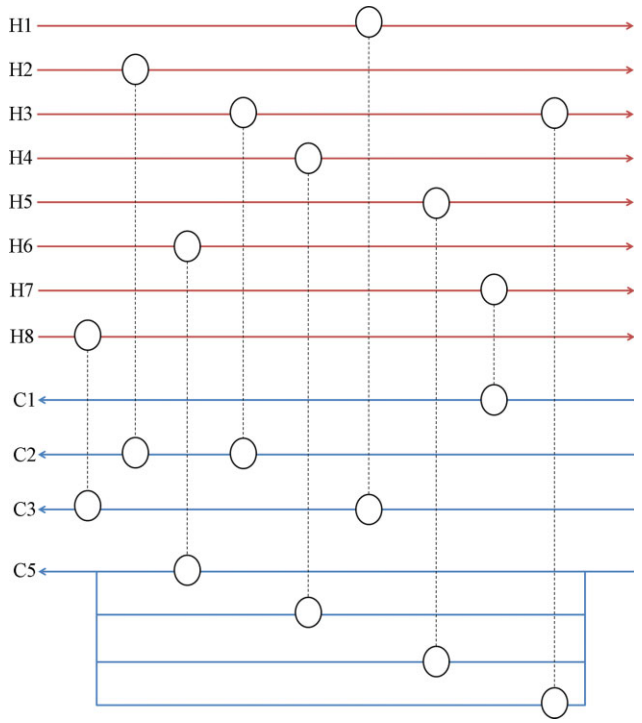

Figure 8. Best heat exchanger network for the LNG plant.

[Color figure can be viewed in the online issue, which is available at www.interscience.wiley.com.]

in Figure 7, the cubic correlations are reasonable approximations for the *T-H* curves for the LNG system. Except for two cases (H5 and H7), cubic correlations completely match the actual *T-H* curves. Note that a proper scaling of *T-H* data is crucial to obtain good approximations. We use $\theta_{ijk} = 3$ K, $F^{L}_{ijk} = f^{L}_{ijk} = 0.05$, and $\eta_{ij} = 1$. Costs of utilities (UC) are taken as \$8000/GJ/h, \$5000/GJ/h, \$10,000/GJ/h, and \$1000/GJ/h for H7, H8, C4, and C5, respectively. The fixed costs (FC) are \$150,00, \$10,000, and \$10,000, and unit-area costs (CA) are \$20, \$30, and \$10 for exchangers, coolers, and heaters, respectively.

F0 (F1) has 1465 (1439) continuous and 468 (90) binary variables, 4017 (3387) constraints, 13,152 (10,254) nonzeros, and 3810 (2298) nonlinear terms. Because of our prior knowledge on some infeasible matches, we are able to eliminate many variables and constraints. BARON gives infeasible solutions for both F0 and F1. The first network obtained by solving F1 using DICOPT satisfies Eq. 14c–f for all exchangers. Therefore, our algorithm does not search further. DICOPT solves three MIP and three NLP sub-problems to find the network in Figure 8 in 2.1 CPUs. A connecting dotted line between the circles of a hot and a cold stream shows the match for each exchanger. The network has three HEs, four coolers, and two heaters, and costs \$550,605. The network with no heat integration has three heaters, and six coolers, and costs \$1,944,039, which is about 3.5 times more expensive. The stream matches, exchanger duties, areas, and inlet/outlet temperatures of each stream are shown in Table 2. H1, H2, and C2 do not require any utility, H3 and C3 use both heat integration and utility, and H4, H5, H6, and C1 use utilities only. C3 is sufficient to precool H1 fully. However, it requires additional heating using H8. C2 is first reboiled by H3, and then H2. H2 needs no more cooling. H3 uses C5 (MR) to achieve its final temperature. H4, H5, and H6 are cooled/liquefied using MR only, and H7 supplies the full reboiling duty of C1. The heater for C1 is an obvious choice, because no heat integration is possible due to its high initial and final temperatures. This allows us to fix the appropriate binary and continuous variables related to exchanges with process streams, but exchanges with hot utilities remain open. Interestingly, C1 is heated completely by H7, which is costlier than H8. Because the fixed costs are the same for all heaters, the main reason behind this is the greater heat transfer area required to heat C1 by H8. Therefore, the selection of utilities is nonintuitive for systems with nonlinear phase changes, and shows the need to allow multiple utilities in GHENS. Among the utilities, C4 is not used at all. H7, H8, and C5 have flows of 1.002, 95.1, and 785.827 Mmol/h. Interestingly, no process stream is split.

Figure 9 shows the PFD of the LNG plant modified based on the network obtained above. We see that NG can be precooled (H1 and H2) and even partially liquefied (H3) by simply using other cold process streams (C3 and C2) from downstream. This saves the use of costly refrigerant. Specifically, the reboiling duty of the nitrogen rejection unit and the heating of cold fuel gas from the same unit can be supplied from the NG precooling and liquefaction section, while the usual practice is to use a pure or mixed refrigerant (such as C4 and C5) to do the same. We used an in-house

Table 2. Final GHEN Data for the LNG Plant

			Hot Stream				Cold Stream			
Match	Exchanger Duty (GJ/h)	Exchanger Area (m^2)	Flow Rate (Mmol/h)	Enthalpy Change (100 MJ/Mmol)	Inlet Temperature (K)	Outlet Temperature (K)	Flow Rate (Mmol/h)	Enthalpy Change (100 MJ/Mmol)	Inlet Temperature (K)	Outlet Temperature (K)
H1-C3	62.16	244.94	25.9	24	290	243	25.68	24.206	109	187.3
H2-C2	26.429	109.53	24.7	10.7	235	218	25	10.572	109.7	115
H3-C2	3.196	13.972	23.3	1.372	218	217.5	25	1.278	109	109.7
H3-C5	76.723	1796.61	23.3	32.928	217.5	198	274.01	2.8	105	110
H4-C5	91.336	3361.42	23.3	39.2	198	155	326.2	2.8	105	110
H5-C5	5.5125	128.194	0.525	105	269	155	19.687	2.8	105	110
H6-C5	46.459	4718.89	23.825	19.5	148	115	165.93	2.8	105	110
H7-C1	0.6413	9.917	1.002	6.4	450	440	0.635	10.1	334	358
H8-C3	41.844	415.31	95.1	4.4	370	365	25.68	16.294	187.3	240

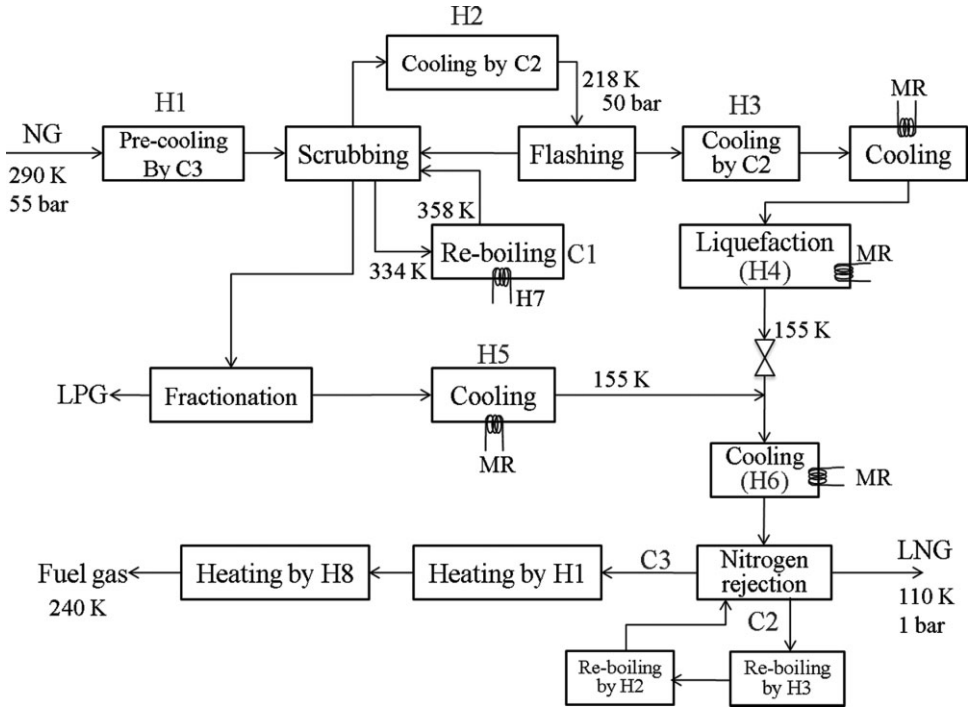

Figure 9. PFD of the LNG plant modified based on our best solution.

simulation of an existing LNG plant as the base to compare our results. Our model results project 15.6% and 9.7% reductions in utility and total annualized cost respectively vs. the base configuration. Because the processing plants for LNG, air separation, ethylene, and other cryogenic gases involve extensive heat exchange and refrigeration, the GHENS methodology developed in this article shows promise for savings in energy and operating costs.

Phenol purification process

A phenol purification process consists of a series of distillation columns. All columns operate under low pressure or vacuum due to concerns related to energy and thermal cracking. The process originally involves four hot and three cold process streams. All of them are mixtures of different compositions of acetone, phenol, cumene, cumyl-phenol, M-Ph ketone, acetal, water and alpha methyl styrene. Depending on the states, these streams are decomposed into six hot (H1-H6) and four cold (C1-C4) single-zone sub-streams. Table 3 gives their temperatures, flows, film heat transfer coefficients, and stream property data. H1, H3, and C2 undergo multicomponent phase changes in reboilers or condensers. The industry practice is to use 25 barg steam in the reboilers and as hot utility, and cooling water or costly refrigerant in the condensers and/or as cold utility. We use one hot utility (saturated steam at 25 barg) and three cold utilities (cooling water, refrigerant, and warm water). Figure 10 shows the fits for the *T-H* curves for all streams and utilities. The cubic correlations almost exactly approximate the *T-H* curves, except for C3 and C4. The maximum deviation among all fits is $\pm 3.76\%$. We use $\theta_{ijk} = 5$ K, $F^{L}_{ijk} = f^{L}_{ijk} =$

Table 3. Stream Data for the Phenol Purification Process

Stream	Flow Rate (kmol/h)	Initial Temperature (K)	Final Temperature (K)	Total Enthalpy Change (MJ/Kmol)	h (KJ/s m^2 K)	Fitted Parameters		
						A	*B*	*C*
H1	515	369.4	338.2	16.81	1.50	1.52599146	0.0791721	−0.0035418
H2	515	338.0	308.0	6.06	0.50	5.19720672	−0.0776393	0.0060937
H3	780	386.7	383.6	38.27	2.50	0.06913268	0.0001917	0.0000031
H4	780	383.6	318.0	12.71	1.10	4.24974828	0.1966202	−0.0195678
H5	390	395.8	333.0	12.00	0.90	5.46525861	−0.0113376	−0.0006658
H6	1000	443.4	393.0	13.40	0.65	3.82122055	0.0122377	−0.0012476
H7	–	500.0	499.0	33.70	0.25	0.03722671	−0.0003153	0.0000027
C1	625	433.1	441.0	2.10	1.00	4.05921662	−0.4250045	0.1349654
C2	625	441.0	446.5	17.00	2.35	0.33924092	−0.0136232	0.0007471
C3	930	333.8	346.8	18.90	1.10	2.82686823	−0.2561033	0.0075623
C4	350	425.0	443.0	29.60	0.70	2.11842007	−0.1118525	0.0020550
C5	–	265.0	270.0	28.00	0.24	0.16334386	0.0016310	−0.0000388
C6	–	303.0	309.0	0.45	0.19	26.1709729	−74.540100	102.248900
C7	–	323.0	333.0	0.80	0.31	9.20344001	12.36275808	−10.030260

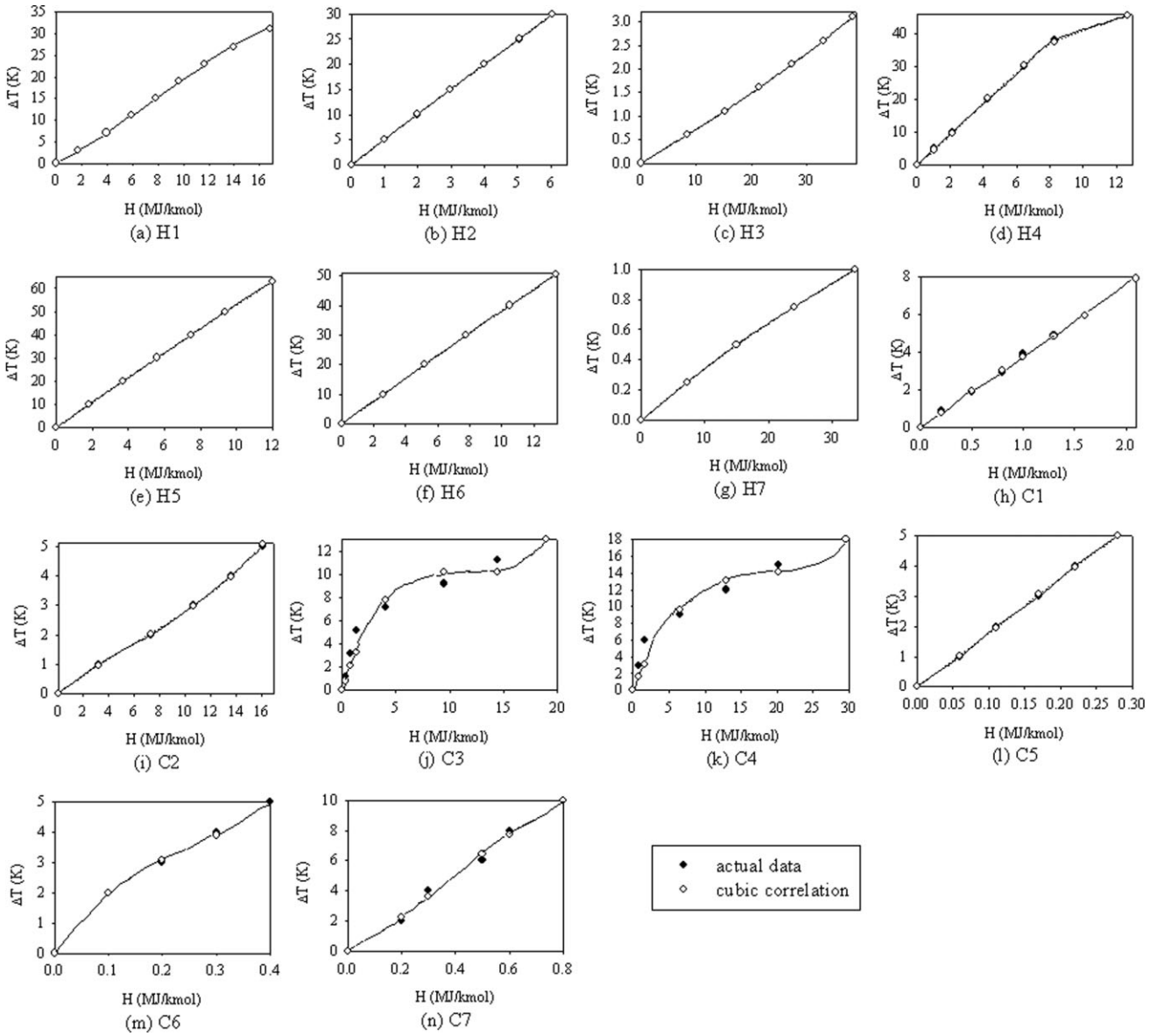

Figure 10. *T-H* curves vs. cubic approximations for streams in the phenol purification process.

0.05, and $\eta_{ij} = 1$. Costs of utilities (UC) are taken as \$50/GJ/h, \$90/GJ/h, \$10/GJ/h, and \$10/GJ/h for H7, C5, C6, and C7. FCs are \$15,000, \$10,000, and \$10,000, and CAs are \$5, \$5, and \$5 for exchangers, coolers, and heaters, respectively.

F0 (F1) has 2075 (1909) continuous and 574 (76) binary variables, 5243 (4413) constraints, 17,275 (13,447) nonzeros, and 5034 (3042) nonlinear terms. Again, due to our prior knowledge on some infeasible matches, we are able to eliminate many variables and constraints. BARON again gives infeasible solutions for both F0 and F1. When we first solve F1 using DICOPT, some exchangers do not satisfy Eq. 14c–f. Therefore, following the procedure in Figure 5, we fix x_{ijk}, increase θ_{ijk} by 1 K, and solve F1 again. However, no feasible solution is found. We eliminate this infeasible configuration by using Eq. 18. We obtain a feasible solution in the second iteration. The algorithm takes 24.8 CPU s for this HEN. Figure 11 shows the final HEN with three HEs, seven coolers, and four heaters. Its annualized cost is \$4,434,039. Table 4 lists the stream matches, exchanger duties, areas, and inlet and outlet temperatures of each stream. The network uses all three cold utilities in various amounts. Unlike the HE network for LNG, several process streams split to exchange heat in parallel. For this process as well, we developed an in-house simulation model of the existing phenol purification plant to compare with the existing plant network. Our model results project a 13.1% reduction in the overall annualized cost vs. the existing configuration.

Note that we used linear cost functions ($\eta_{ij} = 1$) for both case studies. This has indeed simplified our problem considerably from a numerical point of view. Although this may be reasonable for sub-ambient processes, it would surely be more realistic to consider $\eta_{ij} < 1$. We indeed tried to solve the two case studies with $\eta_{ij} = 0.8$ using BARON and DICOPT, but both failed to give feasible solutions for F1,

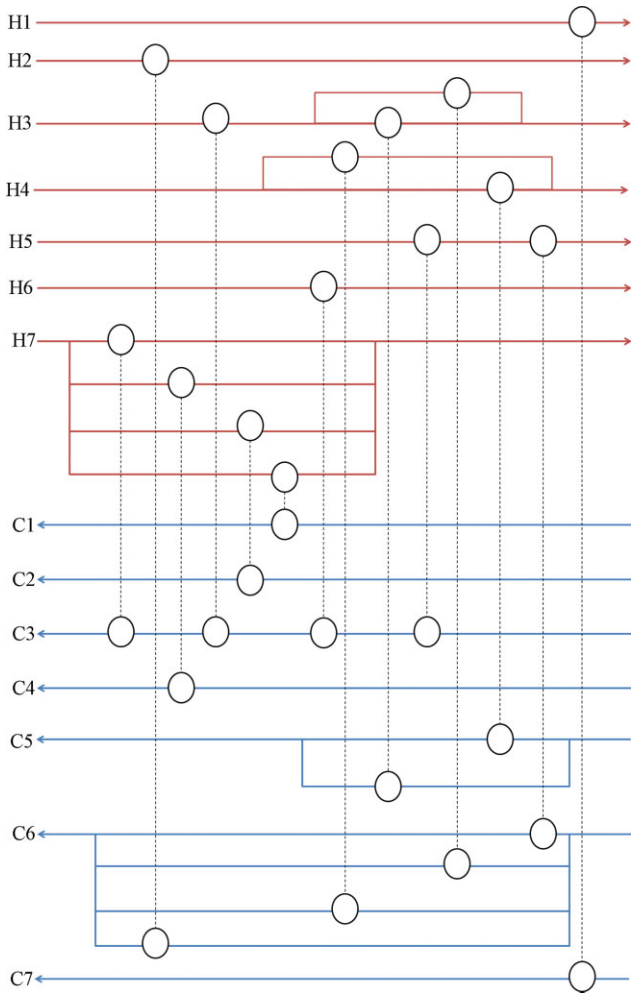

Figure 11. Best heat exchanger network for the phenol purification process.

[Color figure can be viewed in the online issue, which is available at www.interscience.wiley.com.]

which is even simpler than F0. DICOPT could not even solve the first relaxed MINLP problems for the two case studies. Although it is possible to solve much smaller problems, we need a better algorithm for solving larger GHENS problems.

Conclusion

We presented a useful extension of the traditional HENS to accommodate nonisothermal phase changes. The extension enables the inclusion of nonisothermal condensers and reboilers in HENS, and can be used for several applications including energy-intensive processes such as LNG, ethylene, air separation, and other cryogenics. The synthesis model involves a complex, nonconvex mixed-integer nonlinear programming formulation. Some features of our modeling methodology include cubic correlations for *T-H* curves, formulation in terms of enthalpy rather than temperature, analytical treatment of internal MAT points, multiple utility streams, stage bypasses by streams, nonexistent stages, etc. Two real-life case studies project useful reductions in utility and annualized costs compared to existing configurations. One limitation of our methodology is that it only generates a good feasible solution, as the underlying model is nonconvex and highly nonlinear. Much further work is required to achieve better or optimal solutions. However, this work represents our first step towards addressing the challenges associated with generalizing the traditional HENS literature.

Acknowledgments

The authors would like to acknowledge the financial support for this work in the form of a Research Scholarship and a cross-faculty research grant R-279-000-246-123 from the National University of Singapore (NUS), and a research grant (05017P) from a collaborative research project between National University of Singapore (NUS) and Qatar University.

Notation

Indices

s = stream
i = hot stream
j = cold stream
k = stage

Parameters

A_s, B_s, C_s = fitted parameters for *T-H* relations of stream s
h_s = film heat transfer coefficient of stream s

Table 4. Final GHEN Data for Phenol Purification Process

			Hot Stream				Cold Stream			
Match	Exchanger Duty (GJ/h)	Exchanger Area (m^2)	Flow Rate (kmol/h)	Enthalpy Change (MJ/Mmol)	Inlet Temperature (K)	Outlet Temperature (K)	Flow Rate (kmol/h)	Enthalpy Change (MJ/Mmol)	Inlet Temperature (K)	Outlet Temperature (K)
H1-C7	8.657	356.69	515	16.81	369.4	338.2	10821.4	0.8	323	333
H2-C6	3.121	371.48	515	6.06	338	308	6935.3	0.45	303	309
H3-C3	0.746	6.67	780	0.957	386.7	386.6	930	0.802	345.6	346.4
H3-C5	26.119	281.94	700	37.313	386.6	383.6	932.83	28	265	270
H3-C6	2.985	59.57	80	37.313	386.6	383.6	6633.5	0.45	303	309
H4-C5	6.196	111.93	487.5	12.71	383.6	318	221.29	28	265	270
H4-C6	3.718	161.92	292.5	12.71	383.6	318	8261.5	0.45	303	309
H5-C3	3.088	45.48	390	7.918	395.8	355.1	930	3.321	333.8	340.6
H5-C6	1.592	74.38	390	4.082	355.1	333	3537.4	0.45	303	309
H6-C3	13.4	121.66	1000	13.4	443.4	393	930	14.409	340.6	345.6
H7-C1	1.313	29.17	38.95	33.7	500	499	625	2.1	433.1	441
H7-C2	10.625	233.05	315.28	33.7	500	499	625	17	441	446.5
H7-C3	0.343	3.05	10.17	33.7	500	499	930	0.368	346.4	346.8
H7-C4	10.36	249.86	307.42	33.7	500	499	350	29.6	425	443

U_{ij} = overall heat transfer coefficient when hot stream i and cold stream j contacts
θ = minimum approach temperature
F_s = total flow rate of stream s
F_{ijk}^{L} = lower bound of flow rate of split j of stream i in HE_{ijk}
f_{ijk}^{L} = lower bound of flow rate of split i of stream j in HE_{ijk}
TIN_s = initial temperature of stream s
HIN_s = initial enthalpy of stream s
$TOUT_s$ = final temperature of stream s
$HOUT_s$ = final enthalpy of stream s
TR_s = reference temperature of stream s
M, M_1, M_2, M_3 = big numbers
FC_{ij} = fixed cost of installation for the exchanger between stream i and j
UC_s = unit cost of utility s
η = exponent of area cost relation.
CA_{ij} = cost of unit area of the exchanger between stream i and j

Binary variables

x_{ijk} = 1 if hot stream i contacts cold stream j at stage k
α_{ijk1} = 1 if $c_{ijk}^2 \geq 3b_{ijk}d_{ijk}$
α_{ijk2} = 1 if $3b_{ijk} \leq 0$
α_{ijk3} = 1 if $b_{ijk} + 2c_{ijk} + 3d_{ijk} \geq 0$

Continuous variables

F_{ijk} = flow rate of split j of stream i in HE_{ijk}.
f_{ijk} = flow rate of split i of stream j in HE_{ijk}.
T_{ik} (t_{jk}) = temperature of stream i (j) as it leaves (enters) stage k
H_{ik} (h_{jk}) = enthalpy of stream i (j) as it leaves (enters) stage k
Q_{ijk} = heat duty of HE_{ijk}
ΔH_{ijk} = changes in enthalpies per unit mass for hot stream i in HE_{ijk}
Δh_{ijk} = changes in enthalpies per unit mass for cold stream j in HE_{ijk}
T_i (t_j) = temperature of hot (cold) stream i (j)
H_i (h_j) = enthalpy of hot (cold) stream i (j)
z_{ijk} = denotes internal point in HE_{ijk}
a_{ijk}, b_{ijk}, c_{ijk}, d_{ijk} = coefficients of cubic correlation
ATD_{ijk} = average temperature difference in HE_{ijk}

Literature Cited

1. Energy Information Administration/Monthly Energy Review May 2008. Available at:http://www.eia.doe.gov/emeu/mer/consump.html.
2. Zargarzadeh M, Karimi IA, Alfadala HE. Olexan: a tool for online exergy analysis. Presented in ESCAPE17, Bucharest, Romania, May 27–30, 2007.
3. Masso AH, Rudd DF. The synthesis of system designs – II. Heuristic structuring. *AIChE J*. 1969;15:10–17.
4. Gundersen T, Naess L. The synthesis of cost optimal HE networks. An industrial review of the state of the art. *Comput Chem Eng*. 1988;6:503–530.
5. Ježowski J. Heat exchanger network grassroot and retrofit design. The review of the state-of-the-art: Part I. HE network targeting and insight based methods of synthesis. *Hung J Ind Chem*. 1994;22:279–294.
6. Ježowski J. Heat exchanger network grassroot and retrofit design. The review of the state-of-the-art: Part II. HE network synthesis by mathematical methods and approaches for retrofit design. *Hung J Ind Chem*. 1994;22:295–308.
7. Furman KC, Sahinidis NV. A critical review and annotated bibliography for HE network synthesis in the 20th century. *Ind Eng Chem Res*. 2002;40:2335–2370.
8. Hasan MMF, Karimi IA, Alfadala HE. Modeling phase change in HE network synthesis. *In Proceedings of ESCAPE18*, Lyon, France, June 1–4, 2008.
9. Ponce-Ortega JM, Jiménez-Gutiérrez A, Grossmann IE. Optimal synthesis of HE networks involving isothermal process streams. *Comput Chem Eng*. 2008;32:1918–1942.
10. Liporace FS, Pessoa FLP, Queiroz EM. HE network synthesis considering changing phase streams. *Therm Eng*. 2004;3:87–95.
11. Douglas JM. *Conceptual Design of Chemical Processes*. New York: McGraw-Hill, 1988.
12. Castier M, Queiroz E. Energy targeting in HE network synthesis using rigorous physical property calculations. *Ind Eng Chem Res*. 2002;41:1511–1515.
13. Kern DQ. *Process Heat Transfer*. New York: McGraw-Hill, 1950.
14. Linnhoff B. Pinch analysis – A state-of-the-art overview. *Chem Eng Res Des*. 1993;71(A):503–522.
15. Floudas CA, Ciric AR. Strategies for overcoming uncertainties in HE network synthesis. *Comput Chem Eng*. 1989;13:1133–1152.
16. Papoulias SA, Grossmann IE. A structural optimization approach in process synthesis – II. Heat recovery networks. *Comput Chem Eng*. 1983;7:202–721.
17. Floudas CA, Ciric AR, Grossmann IE. Automatic synthesis of optimum HE network configurations. *AIChE J*. 1986;32:276–290.
18. Ciric AR, Floudas CA. HE network synthesis without decomposition. *Comput Chem Eng*. 1991;15:385–396.
19. Yee TF, Grossmann IE. Simultaneous optimization models for heat integration-II. HE network synthesis. *Comput Chem Eng*. 1990;14:1165–1184.
20. Daichent MM, Grossmann IE. Preliminary screening procedure for the MINLP synthesis of process systems–II. HE networks. *Comput Chem Eng*. 1994;18:679–709.
21. Soršak A, Kravanja Z. Simultaneous MINLP synthesis of HE networks comprising different exchanger types. *Comput Chem Eng*. 2002;26:599–615.
22. Hasan MMF, Alfadala HE, Karimi IA, Grootjans H. Modeling and Simulation of Main Cryogenic HE in an LNG Plant. *Presented in AIChE Annual Meeting*, San Francisco, CA, USA, Nov 12–17, 2006.
23. Hasan MMF, Karimi IA, Alfadala HE, Grootjans H. Modeling and simulation of main cryogenic HE in a base-load liquefied natural gas plant. *In Proceedings of ESCAPE17*, 2007, 219–224.
24. Hasan MMF, Karimi IA, Alfadala HE, Grootjans H. Operational modeling of multi-stream HE with phase changes. *AIChE J*. 2009;55:150–171.
25. Furman KC, Sahinidis NV. Computational complexity of HE network synthesis. *Comput Chem Eng*. 2001;25:1371–1390.
26. Floudas CA. *Nonlinear and mixed-integer optimization*. New York: Oxford University Press, 1995.
27. Zamora JM, Grossman IE. A global MINLP optimization algorithm for the HE networks with no stream splits. *Comput Chem Eng*. 1998;22:367–384.
28. Björk KM, Westerlund T. Global optimization of HENS problems with and without the isothermal mixing assumption. *Comput Chem Eng*. 2002;26:1581–1593.
29. Bergamini ML, Scenna NJ, Aguirre PA. Global optimal structures of HE networks by piecewise relaxation. *Ind Eng Chem Res*. 2007;46:1752–1763.
30. Lee GC, Smith R, Zhu XX. Optimal synthesis of mixed-refrigerant systems for low temperature processes. *Ind Eng Chem Res*. 2002;41:5016–5028.
31. Grossmann IE, Viswanathan J, Vecchietti A, Raman R, Kalvelagen E. DICOPT. In: *GAMS: the solver manuals. GAMS Development Corporation*, 2005; Available at: http://www.gams.com/dd/docs/solvers/dicopt.pdf.
32. Sahinidis N, Tawarmalani M. BARON. In: *GAMS: the solver manuals. GAMS Development Corporation*, 2005; Available at: http://www.gams.com/dd/docs/solvers/baron.pdf.
33. Brooke A, Kendrick D, Meeraus A, Raman R.GAMS: a user's guide. GAMS Development Corporation. 2005; Available at: http://www.gams.com/docs/gams/GAMSUsersGuide.pdf.
34. Hasan MMF, Zheng AM, Karimi IA. Minimizing boil-off losses in liquefied natural gas transportation. *Ind Eng Chem Res*. 2009. In press.
35. Aspelund A, Gundersen T. A liquefied energy chain for transport and utilization of natural gas for power production with CO_2 capture and storage–Part 1. *Appl Energ*. 2009;86:781–792.
36. Hasan MMF, Karimi IA, Alfadala HE. *Optimizing compressor operations in an LNG plant*. In: Alfadala HE, Rex Reklaitis GV, El-Halwagi MM, editors. *Proceedings of 1st Annual Gas Processing Symposium*. 2009:179–184.

37. Del Nogal F, Kim JK, Perry S, Smith R. Optimal design of mixed refrigerant cycles. *Ind Eng Chem Res*. 2008;47:8724–8740.
38. Shin MW, Shin D, Choi SH, Yoon ES, Han C. Optimization of the operation of boil-off gas compressors at a liquefied natural gas gasification plant. *Ind Eng Chem Res*. 2007;46:6540–6545.

Appendix: MAT Constraints

Let $g(z) = a + bz + cz^2 + dz^3$ $(-\infty < z < \infty)$ be an arbitrary cubic function. Let ξ be such that,

$$g^* = \min_{0\le z\le 1} g(z) = g(z=\xi)$$

In other words, g^* occurs at $z = \xi$. Clearly, $\xi = 0$ and $\xi = 1$ are two possibilities. Hence, to force $g(z) \ge \theta$ at all $z \in [0,1]$, we must impose,

$$g(0) = a \ge \theta \tag{A1}$$

$$g(1) = a + b + c + d \ge \theta \tag{A2}$$

The third possibility is that g^* occurs at a stationary point of $g(z)$. For this, $g(z)$ must have a stationary point in [0,1], which must be a valid minimum. To identify such a stationary point, we solve $g'(z) = b + 2cz + 3dz^2 = 0$. This gives us $c + 3dz = \pm\sqrt{c^2 - 3bd}$, which has two possible roots. These roots are either both real or both imaginary. If both are real, then $g''(z=\xi) > 0$ tells us that $c + 3d\xi = \sqrt{c^2 - 3bd}$ represents a minimum. For this minimum (represented by ξ) to be within [0,1], the following must hold.

$$c^2 \ge 3bd \tag{A3a}$$

$$b \le 0 \tag{A3b}$$

$$b + 2c + 3d \ge 0 \tag{A3c}$$

Since we want $g(z = \xi) \ge \theta$, we substitute $c + 3dz = \sqrt{c^2 - 3bd}$ in $g(z)$ and simplify to get,

$$9d(3ad - bc) + 2c^3 - 2\left(c^2 - 3bd\right)^{3/2} \ge 27\theta d^2 \tag{A4}$$

Clearly, we need to impose Eq. A4, only if Eq. A3a–c hold. If the constants *a–d* are variables as in our formulation, then this conditional imposition needs binary variables and constraints as follows.

$$\alpha_1 = \begin{cases} 1 & \text{if } c^2 \ge 3bd \\ 0 & \text{otherwise} \end{cases}$$

$$\alpha_2 = \begin{cases} 1 & \text{if } b \le 0 \\ 0 & \text{otherwise} \end{cases}$$

$$\alpha_3 = \begin{cases} 1 & \text{if } b + 2c + 3d \ge 0 \\ 0 & \text{otherwise} \end{cases}$$

$$c^2 - 3bd \le M_1\alpha_1 \tag{A5a}$$

$$-b \le M_2\alpha_2 \tag{A5b}$$

$$b + 2c + 3d \le M_3\alpha_3 \tag{A5c}$$

$$9d(3ad - bc) + 2c^3 - 2\left(c^2 - 3bd\right)^{3/2} - 27\theta d^2 \le M(\alpha_1 + \alpha_2 + \alpha_3 - 2) \tag{A6}$$

where M_1, M_2, M_3, and M are sufficiently large numbers. Any large values for M_1, M_2, M_3, and M are acceptable. One set of values is:

$$M = a^U + b^U + c^U + d^U \tag{A7a}$$

$$M_1 = \left[c^U\right]^2 + 3b^U d^U \tag{A7b}$$

$$M_2 = b^U \tag{A7c}$$

$$M_3 = b^U + 2c^U + 3d^U \tag{A7d}$$

where a^{U}, b^{U}, c^{U}, and d^{U} are the maximum possible values of a_{ijk}, b_{ijk}, c_{ijk}, and d_{ijk}, respectively. For GHENS, they are given as follows.

$$a^{\mathrm{U}}_{ijk} = \mathrm{TR}_i + \sqrt{A_i^2}\mathrm{HIN}_i + \sqrt{B_i^2}\mathrm{HIN}_i^2 + \sqrt{C_i^2}\mathrm{HIN}_i^3 + \left[\mathrm{TR}_j + 2\sqrt{A_j^2}\mathrm{HOUT}_j + 4\sqrt{B_j^2}\mathrm{HOUT}_j^2 + 8\sqrt{C_j^2}\mathrm{HOUT}_j^3\right] \tag{A8a}$$

$$b^{\mathrm{U}}_{ijk} = \left[\sqrt{A_j^2} + 4\sqrt{B_j^2}\mathrm{HOUT}_j + 12\sqrt{C_j^2}\mathrm{HOUT}_j^2\right]\mathrm{HOUT}_j + \left[\sqrt{A_i^2} + 2\sqrt{B_i^2}\mathrm{HIN}_i + 3\sqrt{C_i^2}\mathrm{HIN}_i^2\right]\mathrm{HIN}_i \tag{A8b}$$

$$c^{\mathrm{U}}_{ijk} = \left[\sqrt{B_i^2} + 3\sqrt{C_i^2}\mathrm{HIN}_i\right]\mathrm{HIN}_i^2 + \left[\sqrt{B_j^2} + 6\sqrt{C_j^2}\mathrm{HOUT}_j\right]\mathrm{HOUT}_j^2 \tag{A8c}$$

$$d^{\mathrm{U}}_{ijk} = \max\left[C_j\mathrm{HOUT}_j^3, -C_j\mathrm{HOUT}_j^3, C_j\mathrm{HOUT}_j^3 - C_i\mathrm{HIN}_i^3, C_i\mathrm{HIN}_i^3 - C_j\mathrm{HOUT}_j^3\right] \tag{A8d}$$

Manuscript received Mar. 9, 2009, and revision received Jun. 26, 2009.